Tetratopic bis(4,2':6',4''-terpyridine) and bis(3,2':6',3''-terpyridine) ligands as 4-connecting nodes in 2D-coordination networks and 3D-frameworks.

Catherine E. Housecroft* and Edwin C. Constable

Department of Chemistry, University of Basel, Basel, Switzerland

email: catherine.housecroft@unibas.ch
ORCID:
Catherine E. Housecroft 0000-0002-8074-0089
Edwin C. Constable 0000-0003-4916-4041

Abstract

Ditopic, 4,2':6',4''-terpyridine (4,2':6',4''-tpy) and 3,2':6',3''-terpyridine (3,2':6',3''-tpy) present a divergent *N,N'*-donor set (the central N atom typically being non-coordinated) and are ideal building blocks for the assembly of coordination polymers and networks. The step from ditopic to tetratopic ligands which contain two interconnected 4,2':6',4''-tpy or 3,2':6',3''-tpy metal-binding domains renders the ligand capable of acting as a 4-connecting node and is a successful route to increasing the dimensionality of the assembly. In this short overview, we illustrate the recent development of the use of bis(4,2':6',4''-tpy) and bis(3,2':6',3''-tpy) ligands and compare strategies using either ditopic or tetratopic ligands.

Keywords

3,2':6',3''-terpyridine; 4,2':6',4''-terpyridine; coordination polymer; coordination network; multitopic ligands

Dedication: This overview is dedicated to our good friend and colleague George Newkome in recognition of his innovations and pioneering work in the fields of dendrimers and terpyridine chemistry.

1. Introduction

There are forty-eight isomers of terpyridine, but in practice, it is the coordination chemistry of 2,2':6',2''-terpyridine (tpy, Scheme 1) that dominates the discipline. Although tpy can present multiple metal-binding modes [1], it is ubiquitous as a tridentate, chelating ligand. Octahedral $\{M(tpy)_2\}$ units are favourite building blocks for a wide range of metallomacrocycles and cages, the structures of which can be remarkably complex as a result of a judicious choice of connecting domains. Newkome's work in this field has been inspirational as demonstrated by selected, recently reported architectures [2,3,4]. The incorporation of additional donor functionalities in the 4'-positions of the ligands in a $\{M(tpy)_2\}$ unit generates an 'expanded ligand' (Scheme 1) (Scheme 1) [5] with the potential for the assembly of multinuclear systems [6–12].

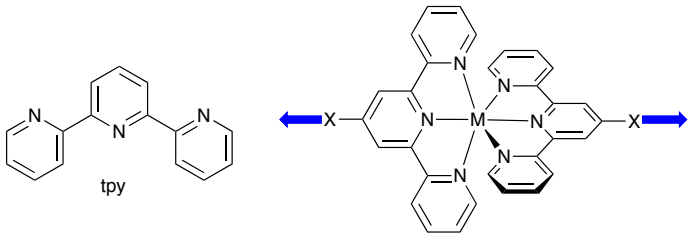

Scheme 1. Structure of 2,2':6',2''-terpyridine and a functionalized $\{M(tpy)_2\}$ motif where X is a donor group, e.g. pyridyl, CO_2^-. The latter acts as a divergent building block in polymer assemblies.

Before continuing, a word about nomenclature. Understanding the partitioning of polydentate ligands into sub-domains with defined coordination properties is the key to the rational design and engineering of coordination polymers and networks. We quantify this information

using the concept of 'metal-binding domains', which are discrete parts of a polydentate ligand which possesses defined coordination properties [13]. If we take 2,2':6',2"-terpyridine in a chelating, tridentate mode as an example (Scheme 2a), it possesses a single metal-binding domain (it binds one metal centre) and is designated as *monotopic*. Of course, other hypodentate [1] bonding modes are possible, but do not concern us here.

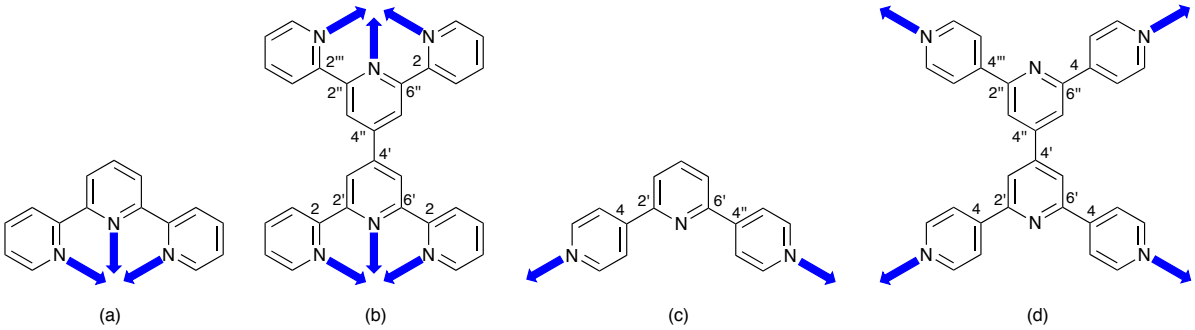

Scheme 2. Definitions of (a) monotopic, (b) and (c) ditopic, and (d) tetratopic ligands.

If we now consider 6,6"-bis(2-pyridyl)-2,2':4',4":2",2"'-quaterpyridine (Scheme 2b), this ligand can present two tridentate tpy metal-binding domains to two metal centres. This ligand is described as *ditopic* because it contains two discrete metal-binding domains. Now let us consider 4,2':6',4"-terpyridine (4,2':6',4"-tpy, Scheme 2c). The first point to note is that this ligand invariably forms hypodentate complexes in which the central ring N1' is not coordinated (see later discussion). The ligand presents two pyridine metal-binding domains to two different metals and, in this bonding mode, is described as *ditopic*. If we extend the discussion to 6,6"-bis(4-pyridyl)-4,2':4',4":2",4"'-quaterpyridine (Scheme 2d), the nitrogen atoms N1' and N1" will not coordinate and so complexes are also hypodentate. In this case, a total of four pyridine metal-binding domains can be presented to a total of four different metal centres and we describe this ligand as *tetratopic*. Note that this nomenclature differs from the description that we have used previously in which we considered ligands of this type as comprising two discrete 4,2':6',4"-tpy domains. In the context of the metal-binding domain

model, 4,2':6',4"-tpy possesses two metal-binding sites and so we have revised the description of ligands containing two 4,2':6',4"-tpy domains to tetratopic.

While multinuclear and polymeric assemblies predicated upon $\{M(tpy)_2\}$ building blocks are attractive, playing the isomer game with terpyridine diversifies the assembly algorithm. Each of 4,2':6',4"-tpy and 3,2':6',3"-terpyridine (3,2':6',3"-tpy) presents a divergent donor set (Scheme 3) in contrast to the convergent set offered by 2,2':6',2"-tpy. By capitalizing upon the synthetic strategies of Kröhnke [14] or Hanan [15], a huge variety of 4'-functionalized 4,2':6',4"-tpy and 3,2':6',3"-tpy ligands is accessible, providing an almost inexhaustible supply of building blocks for the coordination polymer enthusiast. The first reported coordination polymer involving 4,2':6',4"-tpy was $[ZnCl_2(4,2':6',4"\text{-tpy})]_n$ (Fig. 1) [16] and the development of the field has been highlighted in two reviews [17,18]. An inspection of structures (CSD v. 5.38 with updates using Conquest v. 1.19 [19,20]) involving metal complexes of 4,2':6',4"-tpy and 3,2':6',3"-tpy reveals that the ligand typically binds only through the outer nitrogen donors as shown in Scheme 3, although there are a number of structurally characterized examples of hypodentate (monodentate) ligands [21]. Making the transition from 1D-polymers to 2D- or 3D architectures is usually effected by modification of the 4,2':6',4"-tpy and 3,2':6',3"-tpy core. This is most often achieved by the introduction of a coordinatively non-innocent functionality in the 4'-position, for example a carboxylic acid, pyridyl or phosphane group [18], with or without the addition of a co-ligand. Our own strategy has been to design ligands containing multiple 4,2':6',4"-tpy and 3,2':6',3"-tpy domains. At the onset of our investigations, the use of multitopic 2,2':6',2"-tpy ligands was already established [5,22–26] and is a design principle [27,[28]] that has been effectively exploited by Newkome (see above). The assembly of 2D- and 3D-coordination architectures is often depicted as an ensemble of metal nodes and organic linkers, identified through a

topological analysis of the resultant structures [29,30]. Unlike a single divergent 4,2':6',4"-tpy or 3,2':6',3"-tpy unit which function as linkers (as in the (4,4) net in [{$Cd_2(NO_3)_4$(4'-($^nC_5H_{11}O$)-4,2':6',4"-tpy)$_4$}·3$CHCl_3$]$_n$ shown in Fig. 2 [31]), ligands bearing two divergent 4,2':6',4"-tpy or 3,2':6',3"-tpy metal-binding domains have the potential to function as 4-connecting nodes (Scheme 4). The outcome of the combination of metal ion and tetratopic ligand may be determined by both metal and ligand or only by the ligand, depending upon the connectivity of the metal ion within the network. We shall describe examples of both of these scenarios later, as well as an example where the potentially 4-connecting ligand is reduced to a non-nodal role as 2-connecting linker.

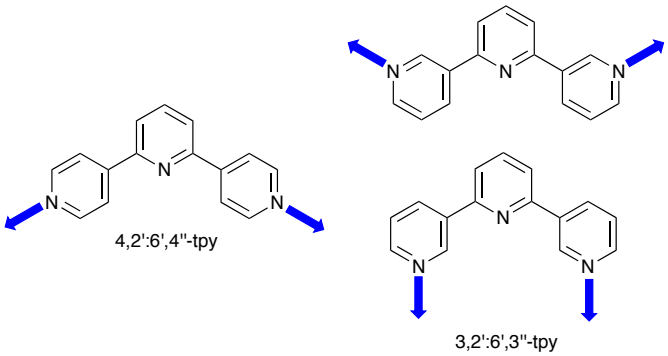

Scheme 3. Divergent bonding modes of 4,2':6',4"-tpy and 3,2':6',3"-tpy. For the latter, rotation about the *trans*-interannular C–C bonds alters the vectorial donor properties of the ligand; two examples are shown.

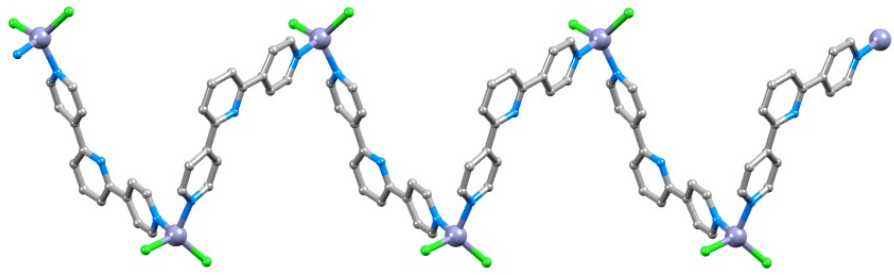

Fig. 1. Part of the 1D-polymer chain in [$ZnCl_2$(4,2':6',4"-tpy)]$_n$ (CSD refcode GAQYUS [16]).

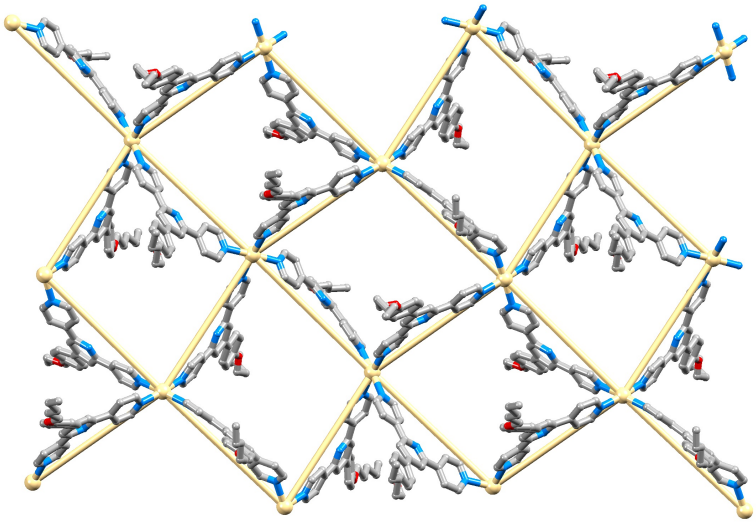

Fig. 2. Part of one (4,4) net in $[\{Cd_2(NO_3)_4(4'\text{-}(^nC_5H_{11}O)\text{-}4,2':6',4''\text{-tpy})_4\}\cdot 3CHCl_3]_n$ (solvent molecules, coordinated nitrate ions and H atoms omitted for clarity) [31].

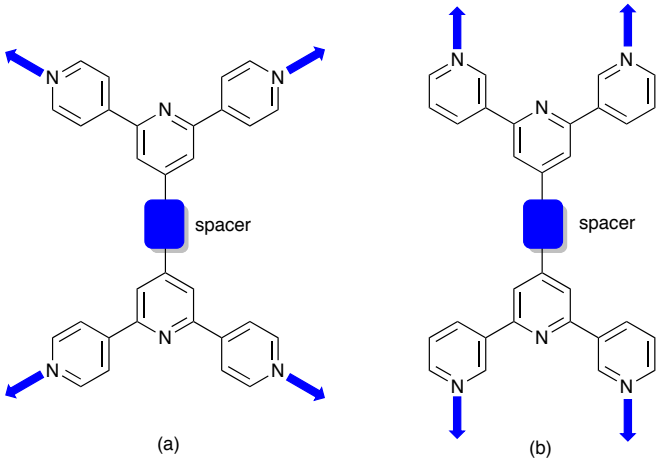

Scheme 4. Tetratopic (a) 4,2':6',4''-tpy and (b) 3,2':6',3''-tpy ligands as 4-connecting nodes.

2. Choice of spacer

In the words of Newkome [2], the "precise control over the shape and size of the architectures is regarded as a tremendous challenge". In the design of ligands with multiple metal-binding domains, the choice of spacer is fundamental to directing the assembly of the coordination network. Prior to 2012 when we embarked on our investigations of tetratopic 4,2':6',4''-tpy and 3,2':6',3''-tpy ligands, reports of such organic molecules were few [32–34] and only one report demonstrated their potential in coordination assemblies. Yoshida *et al.*

have shown that 1,3-bis(4,2':6',4''-terpyridin-4'-yl)benzene (Scheme 5) reacted with cobalt(II) to yield a triply interpenetrating network [34].

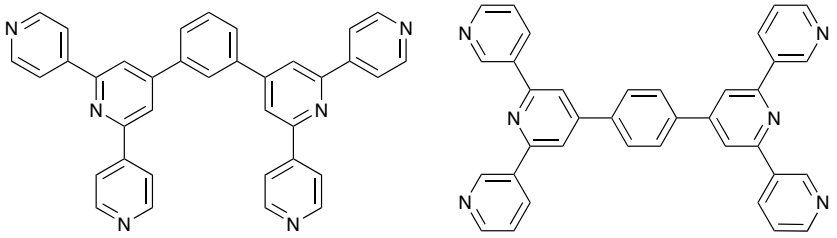

Scheme 5. Structures of 1,3-bis(4,2':6',4''-terpyridin-4'-yl)benzene and 1,4-bis(3,2':6',3''-terpyridin-4'-yl)benzene, reported by Yoshida [34].

For the assembly of coordination polymers and networks, all of our crystal growth experiments are carried out by layering under ambient conditions, and gaining the solubility required for preparation of suitably concentrated solutions is critical. We chose to focus initially upon the incorporation of rod-like spacers between the metal-binding units, with ligand **1** (Scheme 6) being an early target. However, the poor solubility of this compound [35] in common organic solvents led us to move from simple phenylene spacers towards the introduction of solubilizing ^{n}alkoxy chains. Ligand **2** (Scheme 6) fulfilled the requirements of a linear spacer and good solubility [35], and these properties were retained when the chain was significantly shortened in **3** (Scheme 6) [36]. As described later, we have developed a suite of ligands related to **2** and **3**.

The description of **2** and **3** as 'linear' is used to contrast the vectorial disposition of the two 4,2':6',4''-tpy domains with that in Yoshida's ligand (Scheme 7, top left). However, while a 'linear' descriptor is true of the disposition of the central nitrogen donors, as we saw earlier, these are not involved in coordination. When considered as a node in a coordination assembly, ligands such as **2** or **3** are both 4-connecting (Scheme 4), but topographically they

can present limiting planar or pseudo-tetrahedral geometries by virtue of rotational freedom about the spacer–tpy C–C bonds (Scheme 7).

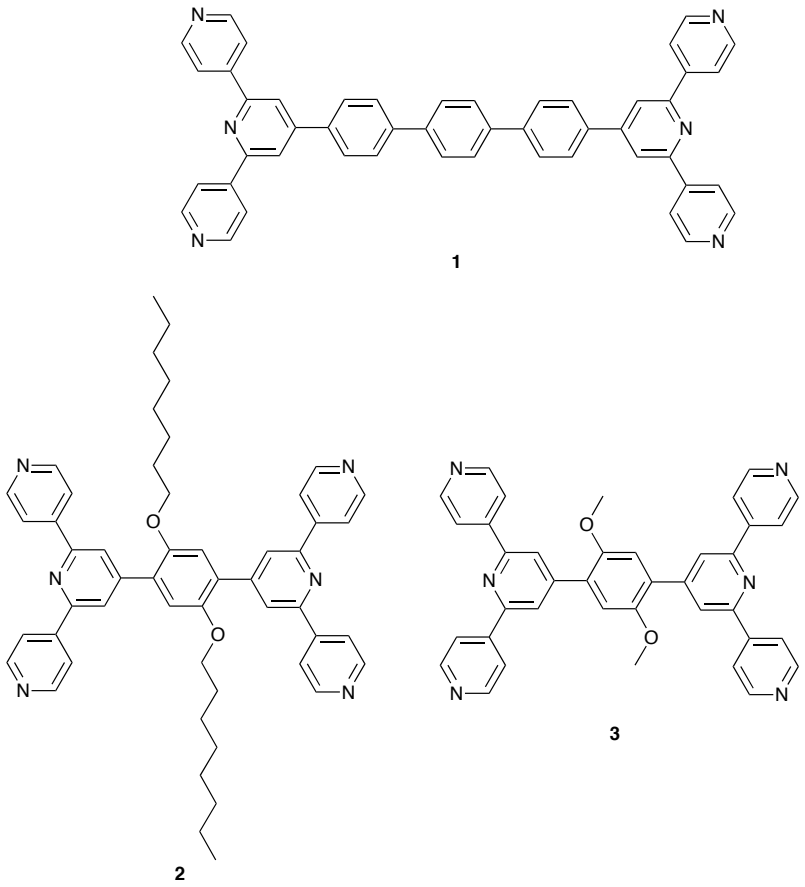

Scheme 6. Structures of ligands **1**–**3**.

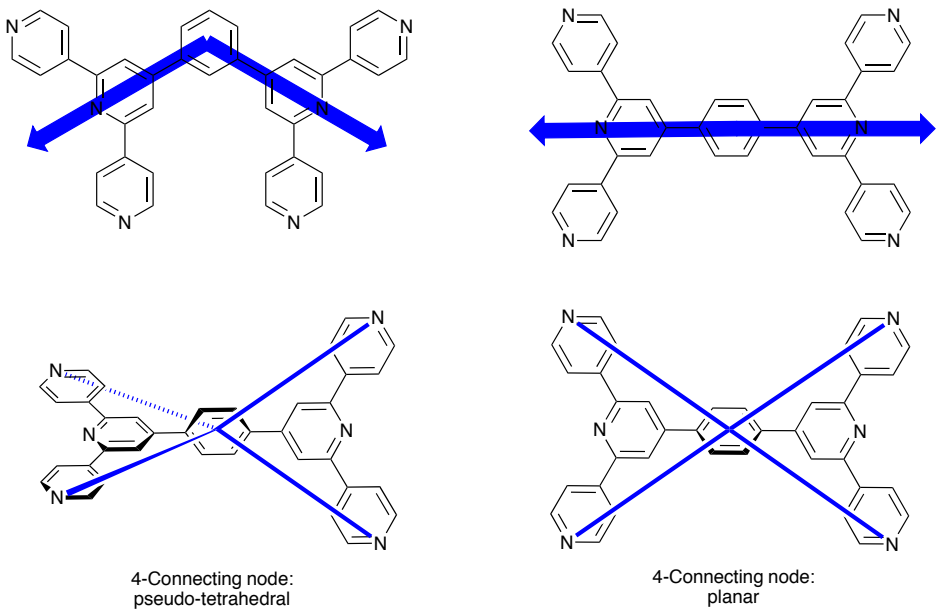

Scheme 7. Top: The 1,3- or 1,4-substitution pattern in the phenylene spacer leads to 'bent' and 'linear' descriptors. Bottom: Rotation about the C–C bonds connecting to the spacer leads to topographically different 4-connecting nodes.

Most of the tetratopic ligands that we discuss in the following sections belong to the same family as **2** and **3** and possess similar degrees of flexibility. Factors that impact on the outcome of the assembly process are the choice of alkoxy substituent and, of course, the metal. In contrast, ligand **4** (Scheme 8) contains a 1,1'-ferrocenyl spacer which exhibits a rotational degree of freedom that can render the 4,2':6',4''-tpy domains cisoid or transoid. Braga *et al*. have shown that the propensity for 1,1'-bis(pyridin-4-yl)ferrocene to adopt a cisoid conformation results in a chelating rather than bridging mode and the assembly of discrete rather than polymeric metal complexes [37,38].

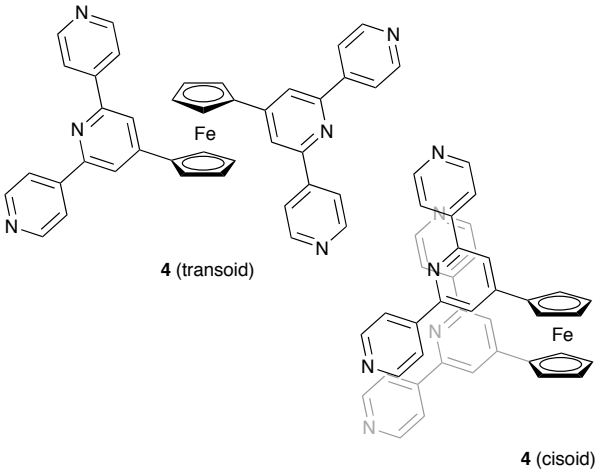

Scheme 8. Structure of ligand **4** showing possible transoid and cisoid conformations.

3. Effects of a tail: from 2D-networks to 3D-frameworks

In this section, we first consider reactions between zinc(II) halides and tetratopic ligands containing two 4,2':6',4''-tpy metal-binding domains and incorporating different alkoxy substituents in the phenylene spacer. Our initial investigation focused on the reaction of $ZnCl_2$ with **2** and this gave rise to the compound $[\{Zn_2Cl_4(\mathbf{2})\}\cdot 4H_2O]_n$ [35]. The zinc(II) centre favours a tetrahedral coordination environment in an $\{ZnN_2Cl_2\}$ coordination sphere, and behaves as a 2-connecting, non-nodal linker in the assembly. The coordination assembly is therefore dictated exclusively by **2** functioning as a 4-connecting node. Given the topographical flexibility of **2** (Scheme 7), the outcome was difficult to predict [39,40]. In $[\{Zn_2Cl_4(\mathbf{2})\}\cdot 4H_2O]_n$, **2** exhibits a planar topography in a uninodal [39] 2D-(4,4) net. Each metallomacrocyclic unit within the net (Fig. 3a) contains two 4,2':6',4''-tpy units from different ligands (coloured red in Fig. 3a) and two 'half-ligands' (coloured orange in Fig. 3a). Figure 3a also defines the nodal connections in one rhombus of the (4,4) net. When the unit in Fig. 3a is viewed down the crystallographic c-axis (Fig. 3b), the origins of the corrugated topography of the net are revealed. Moreover, we see that the ^{n}octoxy chains are directed through the middle of the corrugated sheet. Remarkably, in this and most of the related

structures described below, the ^{n}alkoxy chains are fully ordered, and appear to play a role in stabilizing the assembly. An interesting feature of the coordination architecture is that the rather open and corrugated form of each (4,4)-net permits two sheets to undergo 2D → 2D parallel interpenetration [41,42] as shown in Figs. 3c and 3d. This assembly persists when the chlorido ligands are replaced by bromido ligands in [{Zn_2Br_4(**2**)}]$_n$ [36].

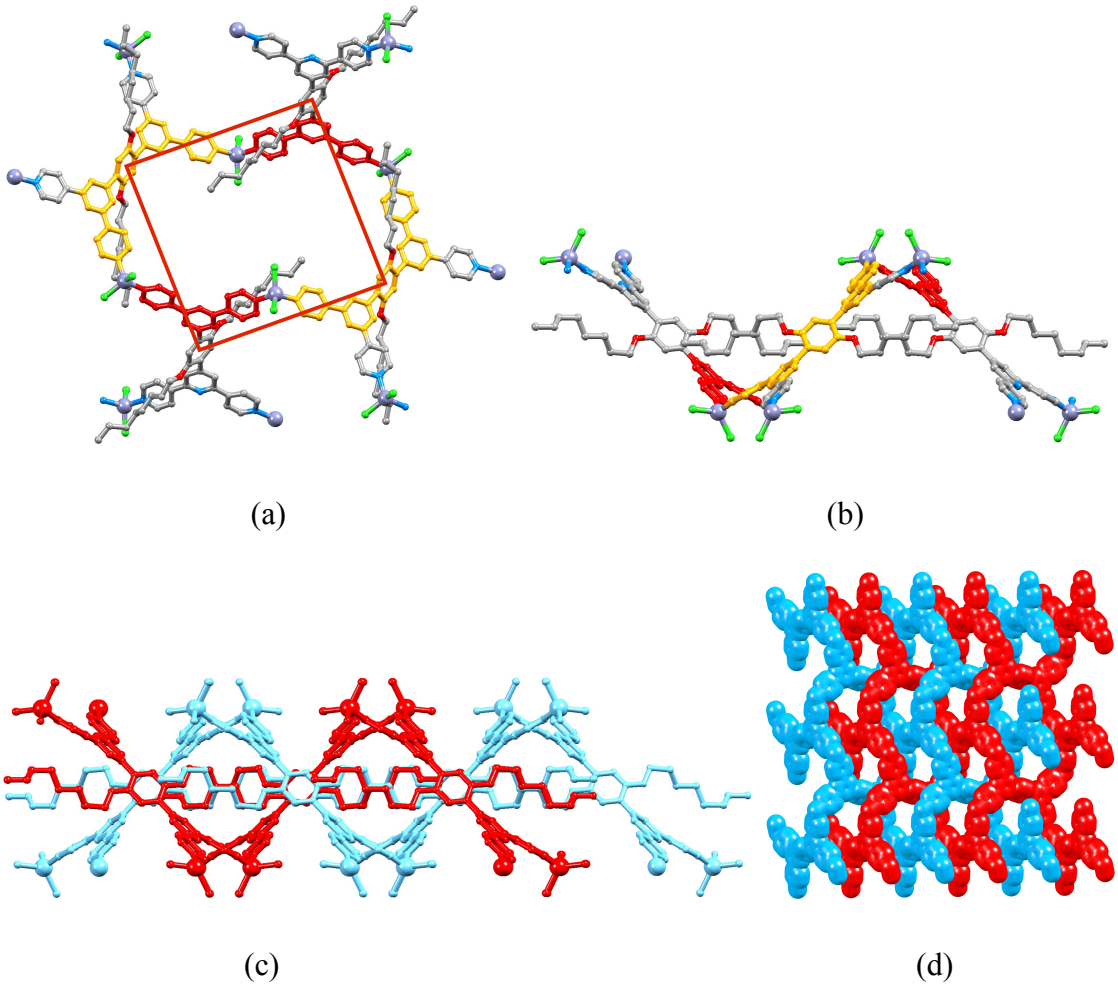

Fig. 3. [{Zn_2Cl_4(**2**)}·$4H_2O$]$_n$: (a) the nodal connections in one unit of the (4,4) net (see text for explanation of the colour-coding in the ligands); (b) the same metallomacrocyclic unit as in (a) viewed down the c-axis; (c) and (d) 2D → 2D parallel interpenetrated nets.

In order to probe the importance of the ^{n}octoxy chains in directing and/or stabilizing the 2D → 2D parallel interpenetrated nets, we investigated the effects of both changing the lengths of the chains (ligands **5** and **6** in Scheme 9) and of essentially removing the chains by replacing ^{n}octoxy by methoxy (ligand **3**, Scheme 6). As previously discussed, absence of a

substituent catastrophically reduces the solubility of the ligand. In the structurally characterized complexes $[\{Zn_2Cl_4(\mathbf{5})\}]_n$ and $[Zn_2Cl_4(\mathbf{6})\cdot 2MeOH]_n$ (Fig. 4), the 2D → 2D parallel interpenetrated nets were again observed [43]. Each of $[\{Zn_2Cl_4(\mathbf{2})\}\cdot 4H_2O]_n$, $[\{Zn_2Br_4(\mathbf{2})\}]_n$, $[\{Zn_2Cl_4(\mathbf{5})\}]_n$ and $[Zn_2Cl_4(\mathbf{6})\cdot 2MeOH]_n$ crystallizes in the *C*2/*c* space group and the unit cell data in Table 1 demonstrate that the structure accommodates an increase in the chain length from ^{n}hexoxy to ^{n}decoxy without significant perturbation of the net itself or of the unit cell parameters. Although reactions of **3** with zinc(II) halides leads once again to 2-dimensional (4,4)-nets, no interpenetration occurs. Instead, $[\{Zn_2Br_4(\mathbf{3})\}\cdot 2C_6H_4Cl_2]_n$ and $[\{Zn_2I_4(\mathbf{3})\}\cdot 2.3C_6H_4Cl_2]_n$ exhibit (4,4)-nets in which the methoxy substituents are directed above and below the sheet (Fig. 5) rather than being directed into the sheet (compare Fig. 5 with Fig. 3b). This observation strongly suggests that the assembly of the 2D → 2D parallel interpenetrated nets relies upon the presence of the long ^{n}alkoxy tails and the stabilization that they deliver to the lattice.

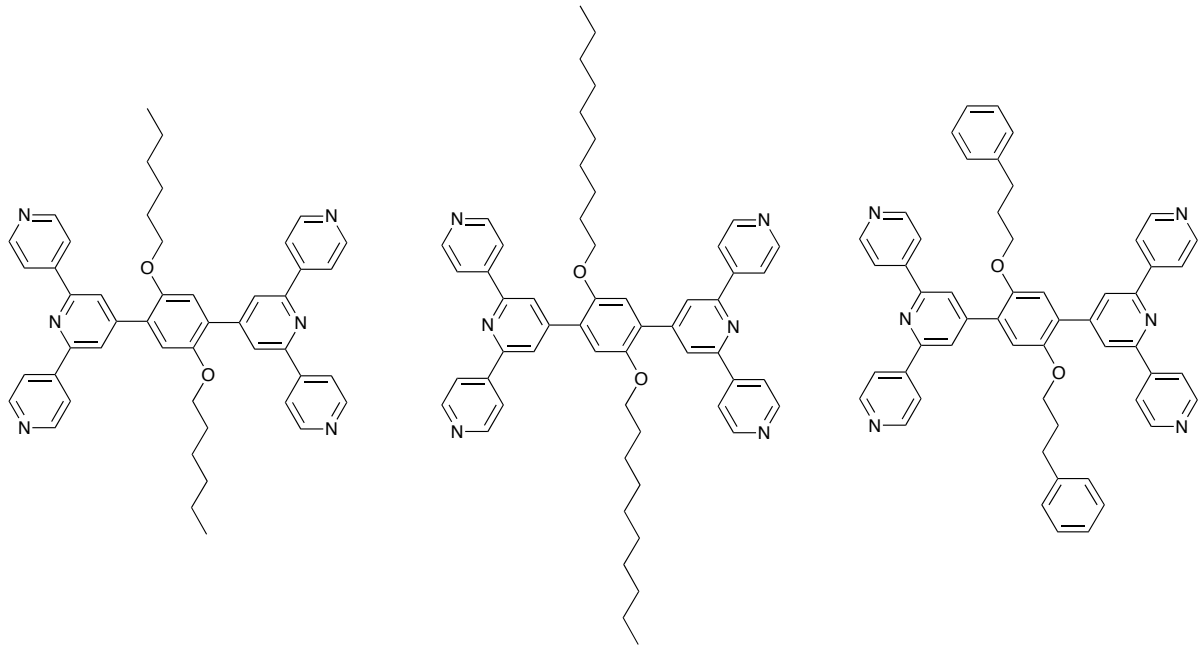

5 **6** **7**

Scheme 9. Structures of tetratopic ligands **5**–**7**.

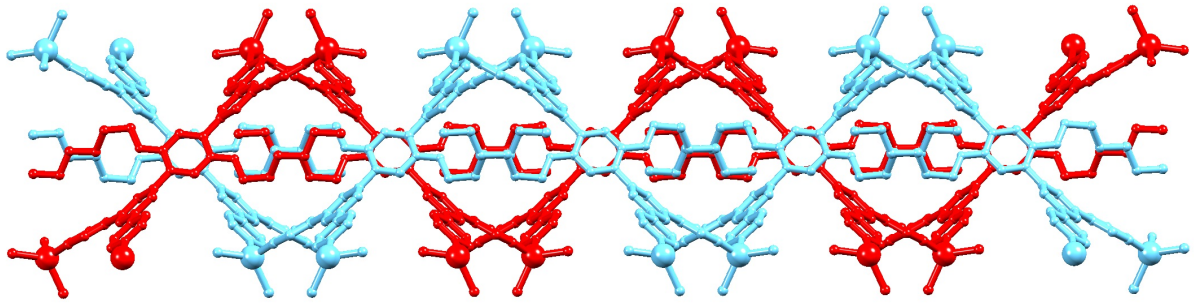

(a)

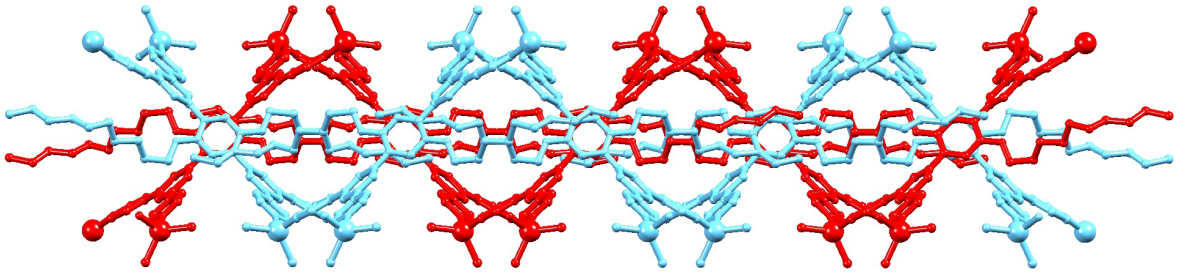

(b)

Fig. 4. 2D → 2D parallel interpenetrated nets in (a) $[Zn_2Cl_4(\mathbf{5})]_n$ and (b) $[Zn_2Cl_4(\mathbf{6})\cdot 2MeOH]_n$. Solvent molecules and H atoms are omitted for clarity.

Table 1 Effects of lengthening of the ^{n}alkoxy tails on unit cell parameters of a series of 2D → 2D parallel interpenetrated nets.

Compound	Alkyl group in the substituent	Space group	*a* / Å	*b* / Å	*c* / Å	*β* / deg	Reference
$[\{Zn_2Cl_4(\mathbf{5})\}]_n$	^{n}hexyl	*C*2/*c*	20.4985(9)	11.6491(3)	23.7457(10)	91.737(4)	[43]
$[\{Zn_2Cl_4(\mathbf{2})\}\cdot 4H_2O]_n$	^{n}octyl	*C*2/*c*	20.6102(6)	11.5999(6)	23.8198(12)	90.978(3)	[35]
$[\{Zn_2Br_4(\mathbf{2})\}]_n$	^{n}octyl	*C*2/*c*	20.6639(16)	11.9145(10)	23.6388(17)	92.289(5)	[36]
$[Zn_2Cl_4(\mathbf{6})\cdot 2MeOH]_n$	^{n}decyl	*C*2/*c*	20.777(2)	11.6382(9)	23.8738(17)	90.074(7)	[43]

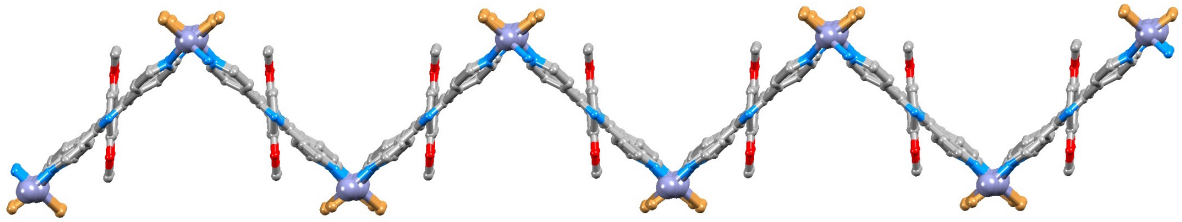

Fig. 5. Part of one corrugated sheet in $[\{Zn_2Br_4(\mathbf{3})\}\cdot 2C_6H_4Cl_2]_n$ (solvent molecules and H atoms omitted).

With the aim of introducing a structural motif that could redirect the assembly from the persistent 2D → 2D parallel interpenetrated nets favoured by the long tails, we focused attention upon a 3-phenyl-^{n}propoxy substituent in ligand **7** (Scheme 9) [43]. This is similar in length to an ^{n}hexoxy tail but incorporates a terminal phenyl group capable of additional arene...arene π-stacking interactions. The outcome was both unexpected and pleasing. Zinc(II) bromide reacts with **7** to yield $[Zn_2Br_4(\mathbf{7})\cdot H_2O]_n$. Just as in the structures described above with **2**, **3**, **5** and **6**, ligand **7** acts as a 4-connecting node with a planar topography while the zinc(II) centres are non-nodal 2-connecting linkers. However, in stark contrast to the earlier structures (Figs. 3–5), $[Zn_2Br_4(\mathbf{7})\cdot H_2O]_n$ crystallizes in the trigonal *R*–3 space group and possesses a 3D architecture consisting of 2-fold interpenetrating $\{6^4.8^2\}$ **nbo** nets (Fig. 6a). As a consequence of the *R*–3 symmetry, the metal-organic framework (MOF) contains hexagonal channels running parallel to the crystallographic *c*-axis. Although not optimal in terms of aromatic ring orientations, stacking interactions between the terminal phenyl rings of the 3-phenyl-^{n}propoxy substituents and 4,2':6',4''-tpy domains in an adjacent net lock the interpenetrated frameworks closely together. As a result, the solvent accessible void space in the lattice is huge (~65% of the total volume) as depicted in Fig. 6b. Significantly, this feature of the assembly in the *R*–3 space group is reminiscent of observations made in the porous MOFs $[Cu(HL)_2]_n$ (H_2L = 1*H*-indazole-5-carboxylic acid) [44] and $[Cu(pmc)_2]_n$ (Hpmc = pyrimidine-5-carboxylic acid) [45].

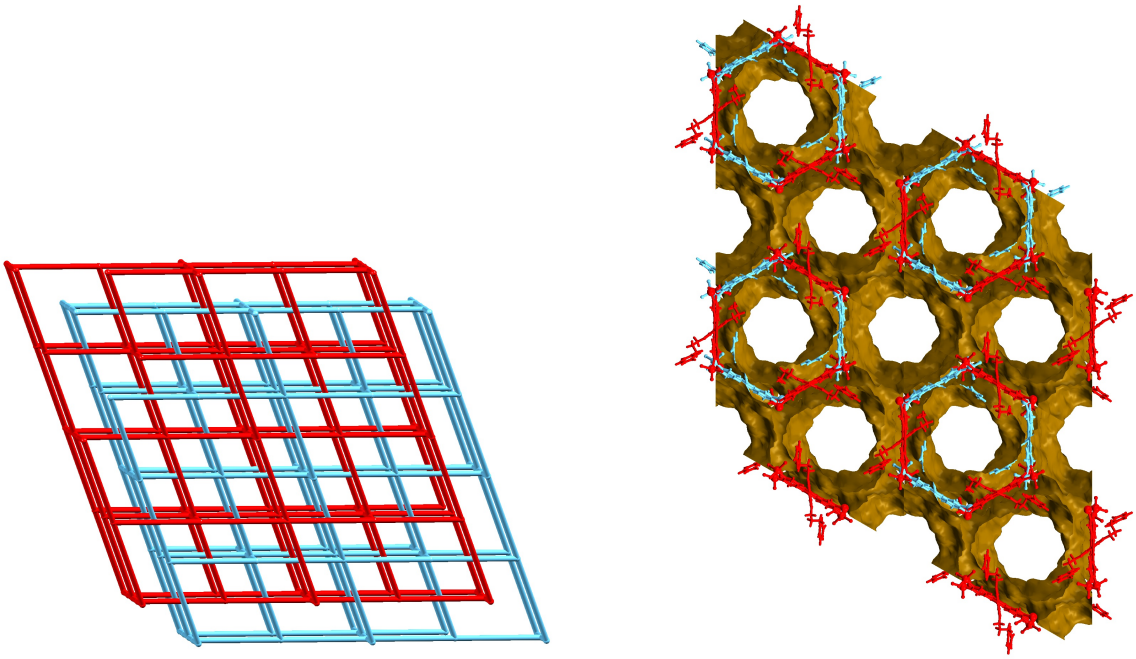

(a) (b)

Fig. 6. (a) TOPOS [46] representation of the interpenetrating **nbo** nets in $[Zn_2Br_4(\mathbf{7})\cdot H_2O]_n$. (b) View down the *c*-axis showing the interpenetrated nets (pale blue and red) and void space in the hexagonal channels (voids displayed using Mercury v. 3.7 [19,47]).

Before leaving this discussion of ^{n}alkoxy-functionalized bis(4,2':6',4"-tpy) ligands, we again emphasize that the assembly is dominated by the 4-connecting ligand node. With two halido ligands, tetrahedral zinc(II) only functions as a linker. We can switch the roles of metal and ligand by choosing a metal that can act as a 4-connecting node and a ditopic 4,2':6',4"-tpy or 3,2':6',3"-tpy that functions as a 2-connecting linker. An instructive example is the reaction of ligand **8** (Scheme 10) with $Co(NCS)_2$ which gives $[Co_2(NCS)_4(\mathbf{8})_4]_n$. The coordination geometry of each cobalt(II) is octahedral with *trans*-thiocyanato ligands, and pairs of adjacent Co atoms in the assembly are bridged by ligand **8**, coordinating through its outer *N*-donors. The structure propagates into a 3D chiral **neb** net, with the 4-connected framework being assembled from 6^6 cage units (Fig. 7) [48]. While ligand **9** (the ^{n}nonoxy analogue of **8**) also combines with $Co(NCS)_2$ to produce a chiral **neb** net [48], ligands **10**, **11** and **12** (Scheme 10) with shorter ^{n}alkoxy functionalities react with $Co(NCS)_2$ to give

[{$Co_2(NCS)_4$(**10**)$_4$}·2$CHCl_3$·1.5MeOH]$_n$, [{$Co(NCS)_2$(**11**)$_2$}·4$CHCl_3$]$_n$ and [{$Co(NCS)_2$(**12**)$_2$}·4$CHCl_3$]$_n$ all of which exhibit 2D (4,4) nets (Fig. 8) [49]. Interestingly, along the series of compounds there is a change in the packing of the (4,4) sheets on going from the methoxy to ethoxy or ^{n}propoxy functionalities. Once again, it appears that the length of the ^{n}alkoxy tail is a significant factor is controlling the coordination network assembly.

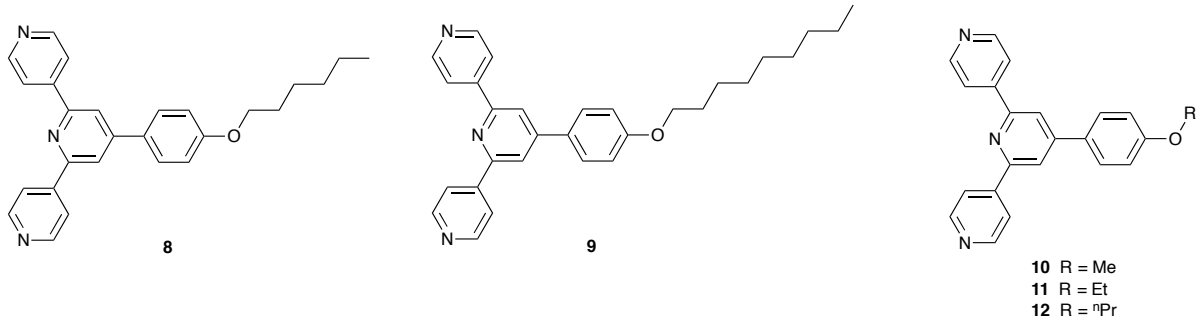

Scheme 10. The structures of ditopic ligands **8**–**12**.

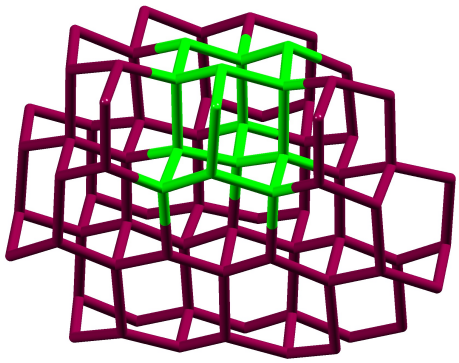

Fig. 7. TOPOS [46] representation of part of the chiral **neb** net in [$Co_2(NCS)_4$(**8**)$_4$]$_n$; the 6^6 cage unit that defines the **neb** net is highlighted in green.

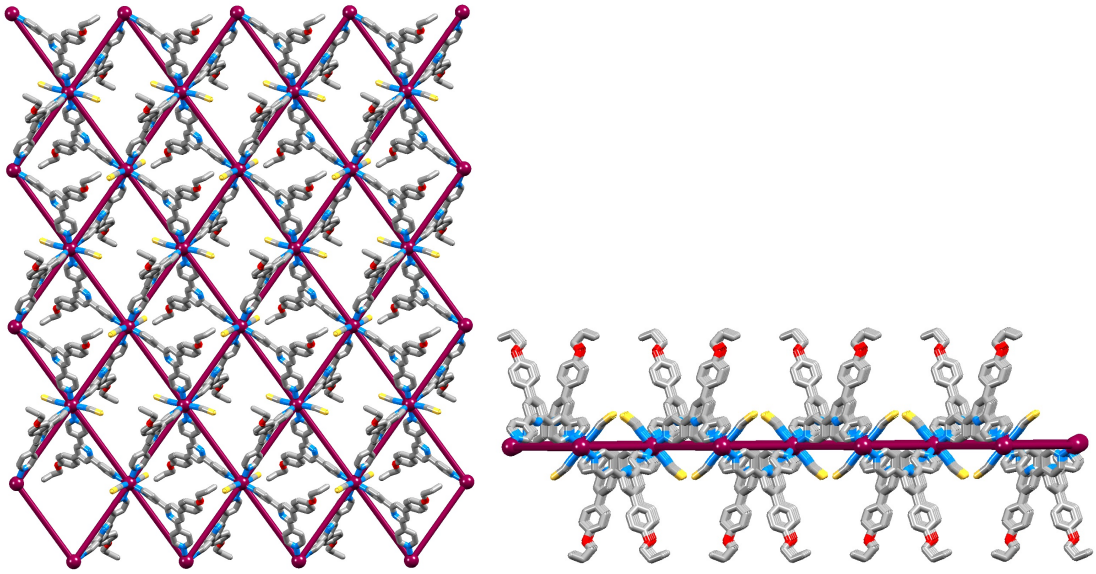

Fig. 8. TOPOS/Mercury [19,46,47] representations of part of one (4,4) net in $[\{Co(NCS)_2(\mathbf{12})_2\}\cdot 4CHCl_3]_n$ (solvent molecules and H atoms omitted).

Following the above discussion, the question arises of what happens if we combine both metal 4-connecting and ligand 4-connecting nodes. The reaction of tetratopic ligand **13** (Scheme 11) with $Co(NCS)_2$ to give $[\{Co(NCS)_2(\mathbf{13})_2\}\cdot 2C_6H_4Cl_2]_n$ provides an instructive example [50]. As shown in Fig. 9a, both the cobalt(II) centres and ligands act as 4-connecting nodes with planar topographies. Propagation of the unit shown in Fig. 9a leads to a 3D **cds** ($6^5.8$) net (Fig. 9b). This differs from the **nbo** ($6^4.8^2$) net (in which adjacent nodes are all mutually perpendicular) in having half of the adjacent nodes mutually perpendicular to one another and half coplanar. Note that in $[Zn_2Br_4(\mathbf{7})\cdot H_2O]_n$, doubly interpenetrating **nbo** nets assembled and were directed only by the 4-connecting ligand **7** node (Fig. 6).

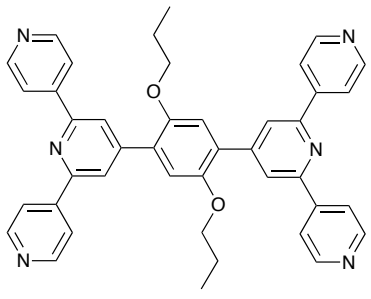

13

Scheme 11. Structure of tetratopic ligand **13**.

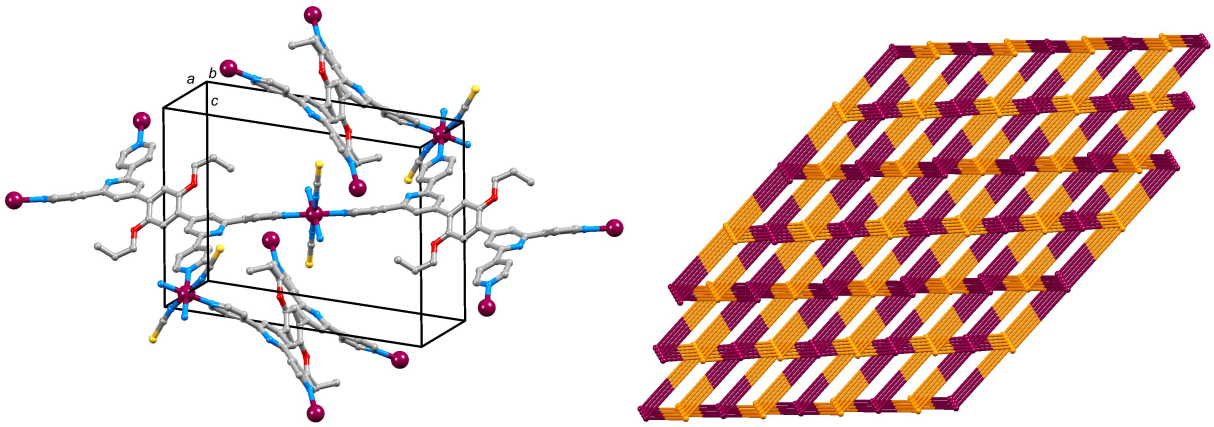

(a) (b)

Fig. 9. [{Co(NCS)$_2$(**13**)$_2$}·2C$_6$H$_4$Cl$_2$]$_n$: (a) Contents of the unit cell (solvent molecules and H atoms omitted) with symmmetry generated atoms. (b) TOPOS [46] representation of part of the **cds** net with Co nodes shown in maroon and ligand nodes in orange.

4. The isomer game: from a bis(4,2':6',4''-tpy) to a bis(3,2':6',3''-tpy) building block

Investigations of tetratopic bis(3,2':6',3''-terpyridine) ligands (Scheme 4b) are still few. In 2013, Yoshida *et al.* reported the formation of a 2D (4,4) network when 1,4-bis(3,2':6',3''-terpyridin-4'-yl)benzene (Scheme 5) was combined with [Co(CNacac)$_2$] (H(CNacac) = 3-cyanopentane-2,4-dione) [34]. The {Co(CNacac)$_2$} unit accepts two *N*-donors from different 3,2':6',3''-tpy ligands into axial sites, thereby acting as a non-nodal 2-connecting linker in the assembly. Figure 10a illustrates that the metallomacrocyclic units that make up the (4,4) net are similar to those shown in Fig. 3s for [{Zn$_2$Cl$_4$(**2**)}·4H$_2$O]$_n$ in that they incorporate two 3,2':6',3''-tpy units from different ligands (coloured red in Fig. 10a) and two 'half-ligands' (coloured orange in Fig. 10a). Note that each 3,2':6',3''-tpy unit adopts a conformation midway between those shown in Scheme 3, reinforcing the flexibility of the binding modes of this domain. When [Co(CNacac)$_2$] was replaced by [Co(dpd)$_2$] (Hdpd = 1,3-diphenylpropane-1,3-dione) in the reaction with 1,4-bis(3,2':6',3''-terpyridin-4'-yl)benzene, a 1D-coordination polymer was observed in which only one *N*-donor of each 3,2':6',3''-tpy unit

was bound to cobalt (Fig. 10b). Steric hindrance originating from the four phenyl substituents in the $\{Co(dpd)_2\}$ unit was suggested as a possible explanation for 1,4-bis(3,2':6',3''-terpyridin-4'-yl)benzene failing to act as a 4-connecting mode [34].

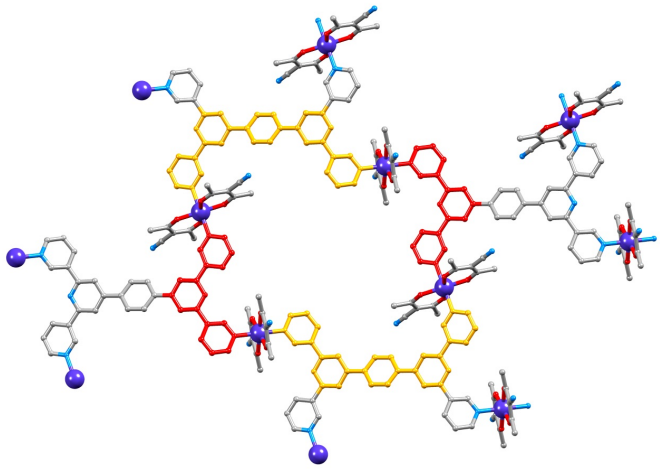

(a)

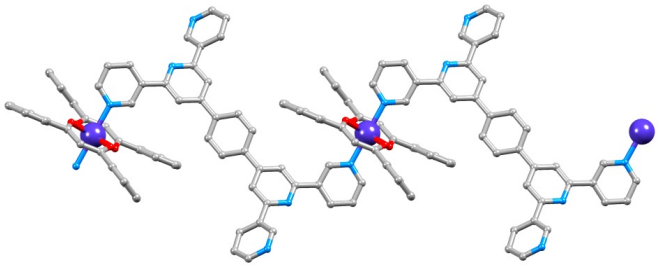

(b)

Fig. 10. (a) One metallomacrocyclic unit in a (4,4) net in $[\{Co_2(CNacac)_4(L)\}\cdot C_2H_2Cl_4]_n$ (L = 1,4-bis(3,2':6',3''-terpyridin-4'-yl)benzene, CSD refcode DEXVIN); see text for explanation of red/orange colouring of the ligands. (b) Part of one 1D-polymer chain in $[\{Co(dpd)_2(L)\}\cdot C_2H_2Cl_4]_n$; solvent molecules and H atoms are omitted. From the work of Yoshida *et al*. [34].

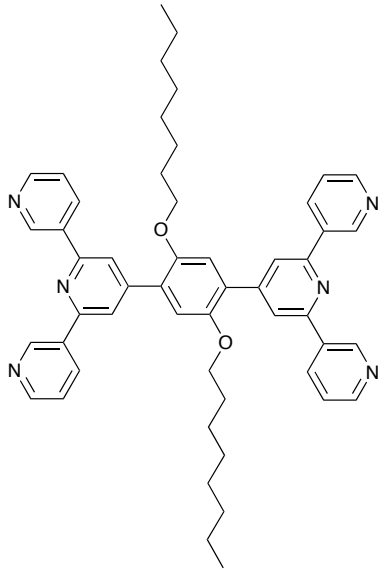

14

Scheme 12. The structure of tetratopic ligand **14** which contains 3,2':6',3''-tpy metal-binding domains.

Ligand **14** (Scheme 12) combines the ^{n}octoxy tails of **2** with two 3,2':6',3''-tpy domains. The combination of either **2** or **14** with $Co(CNS)_2$ is intriguing, given the propensity for $Co(NCS)_2$ to provide a topographically planar 4-connecting metal node (see above) and the ability (in principle) of either **2** or **14** to act as a topographically planar or pseudo-tetrahedral 4-connecting node. Li *et al.* have provided a valuable survey of MOFs based upon 4-connected nodes [40]. Under ambient conditions of crystal growth by layering, a combination of **14** and $Co(NCS)_2$ led to the formation of $[Co(NCS)_2(\mathbf{14})\cdot 4CHCl_3]_n$ which exhibits a 3D $\{4^2.8^4\}$ **lvt** net (Fig. 11). This topology is quite rare among 4-connected nets in MOFs. In $[Co(NCS)_2(\mathbf{14})\cdot 4CHCl_3]_n$, the *trans*-thiocyanato ligands lead to cobalt as a planar node, while rotation about the phenyl-pyridine C–C bonds in **14** makes the ligand a pseudo-tetrahedral node. In contrast to the extended conformations of the ^{n}octoxy and other long tails that appear important in stabilizing some of the architectures described above, those in $[Co(NCS)_2(\mathbf{14})\cdot 4CHCl_3]_n$ are partially folded and the tails occupy the voids in the framework [51]. To date, we have not obtained good quality X-ray diffraction data from crystals grown

from a combination of **2** and $Co(NCS)_2$, although a comparison of this system with that of **14** and $Co(NCS)_2$ remains a focus of our attention.

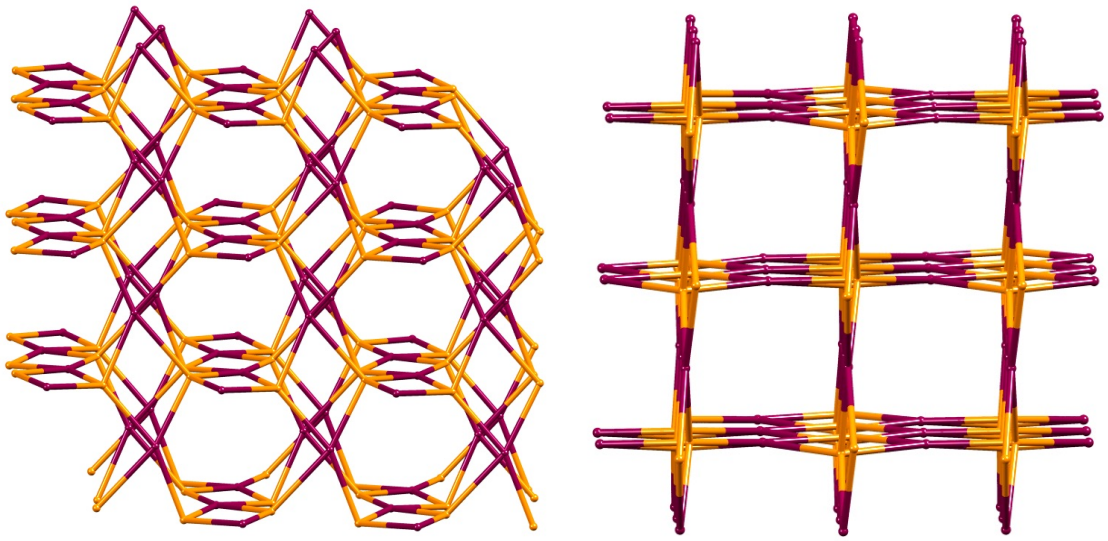

(a) (b)

Fig. 11. Two views of the $\{4^2.8^4\}$ **lvt** net in $[Co(NCS)_2(\mathbf{14})\cdot 4CHCl_3]_n$. The Co nodes are shown in maroon and ligand nodes in orange.

5. Rotational freedom: introducing a 1,1'-ferrocenyl spacer

As discussed earlier, the introduction of a 1,1'-ferrocenyl spacer between the divergent tpy domains (either 4,2':6',4"-tpy or 3,2':6',3"-tpy) introduces a degree of rotational flexibility not present in compounds **2**, **3**, **5–7** or **13**. As an entry into this area, we investigated the coordination behaviour of ligand **4** (Scheme 8) with $ZnCl_2$. A disadvantage of **4** is its low solubility in solvents such as $CHCl_3$. Nonetheless, crystals of $[\{Zn_2(\mathbf{4})Cl_4\}\cdot 3CHCl_3]_n$ were obtained and a preference for a cisoid conformation of **4** results in 'folded' ligands that are connected by zinc(II) linkers (Fig. 12). The favoured cisoid conformation precludes ligand **4** from acting as a 4-connecting node in $[\{Zn_2(\mathbf{4})Cl_4\}\cdot 3CHCl_3]_n$, and the Fe atoms are reduced to being linkers in a 1D-assembly. The 1D-coordination polymer is a double-stranded chain, ligand **4** being the bridge that links the strands. Although multiply-stranded chains containing

4,2':6',4"-tpy domains are known, they differ from $[\{Zn_2(\mathbf{4})Cl_4\}\cdot 3CHCl_3]_n$ in having ditopic ligands supporting each strand and multinuclear metal-containing units connecting the strands, e.g. $[Cd_2(OAc)_4(4'\text{-(biphenyl-4-yl)-4,2':6',4"-tpy})_2]_n$ [52], $[Mn_3(OAc)_6(4'\text{-}(4\text{-}BrC_6H_4)\text{-}4,2':6',4"\text{-tpy})_3]_n$ [53] and $[\{Zn_5(OAc)_{10}(4'\text{-(pentafluorobiphenyl-4-yl)-4,2':6',4"-tpy})\}\cdot 11H_2O]_n$ [54].

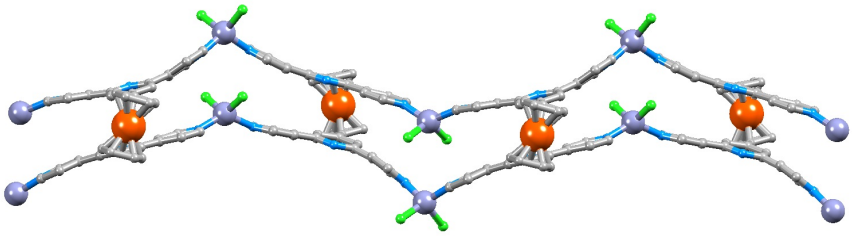

Fig. 12. Part of one double-stranded chain in $[\{Zn_2(\mathbf{4})Cl_4\}\cdot 3CHCl_3]_n$. Solvent molecules and H atoms are omitted.

The introduction of a ferrocenyl substituent in the 4'-position of 4,2':6',4"-tpy or 3,2':6',3"-tpy ligands has another advantage in terms of directing and/or stabilizing coordination assemblies: π-stacking interactions involving ferrocenyl and pyridine units [55]. In addition, it introduces redox-active centres to the coordination assembly [56]. While the coordination behaviour of the ditopic 1-(4,2':6',4"-terpyridin-4'-yl)ferrocene and 1-(3,2':6',3"-terpyridin-4'-yl)ferrocene has been the focus of some attention [50,55,57], that of related tetratopic ligands such as **4** remain virtually unexplored.

6. Conclusions

The divergent *N,N′*-donor set presented by 4,2':6',4"-tpy or 3,2':6',3"-tpy makes these ligands excellent building blocks for the assembly of coordination polymers and networks. Nonetheless, without peripheral functionalization with a donor group, ditopic 4,2':6',4"-tpy or 3,2':6',3"-tpy ligands are limited to roles as 2-connecting linkers. On the other hand, tetratopic ligands with two 4,2':6',4"-tpy or 3,2':6',3"-tpy domains are valuable 4-connecting nodes in

the coordination chemist's toolkit. The introduction of ^{n}alkoxy tails into the spacer between the metal-binding domains not only aids solubility of the ligands, but provides a means of tuning the assembly. Zinc(II) halides react with bis(4,2':6',4''-tpy) ligands to give 2D → 2D parallel interpenetrated (4,4) nets if the ^{n}alkoxy tails are long, but only a simple (4,4) net when methoxy substituents are present. By introducing a terminal phenyl group to the tail, the assembly is switched to 2-fold interpenetrating $\{6^4.8^2\}$ **nbo** nets as exemplified in $[Zn_2Br_4(\mathbf{7})\cdot H_2O]_n$. Changing the metal salt to $Co(NCS)_2$ gives a combination of both metal and ligand 4-connecting nodes, and the assembly of a 3D **cds** ($6^5.8$) net is illustrated with $[\{Co(NCS)_2(\mathbf{13})_2\}\cdot 2C_6H_4Cl_2]_n$. A switch to a tetratopic bis(3,2':6',3''-tpy) ligand alters the vectorial properties of the donor set and reaction of **14** and $Co(NCS)_2$ leads to $[Co(NCS)_2(\mathbf{14})\cdot 4CHCl_3]_n$ with a 3D $\{4^2.8^4\}$ **lvt** net. However, achieving 3D networks is not the exclusive realm of tetratopic ligands. Unexpectedly, $[Co_2(NCS)_4(\mathbf{8})_4]_n$ exhibits a 3D chiral **neb** net even though **8** is ditopic. However, again, the long ^{n}alkyoxy substituents in **8** appear to be important since significant reduction in the tail length leads to simple 2D (4,4) nets in reactions of the bis(4,2':6',4''-tpy) ligands with $Co(NCS)_2$. Finally, introducing the rotationally flexible 1,1'-ferrocenyl spacer between two 4,2':6',4''-tpy metal binding domains has potential for ligands with either cisoid or transoid conformations. Where cisoid is favoured, the potentially 4-connecting ligand is reduced to a role as a 2-connecting linker in the 1D-coordination polymer $[\{Zn_2(\mathbf{4})Cl_4\}\cdot 3CHCl_3]_n$.

There are still only a few coordination networks that employ tetratopic bis(4,2':6',4''-tpy) or bis(3,2':6',3''-tpy) ligands as building blocks. The diverse nature of the assemblies described in this overview points to a rich future and an exciting playground for oligopyridine devotees.

Acknowledgements

The work presented in this overview would not have been possible without the support of the Swiss National Science Foundation (Grant numbers 200020_149067 and 200020_162631) and the University of Basel. Naturally, no results would have been achieved without the enthusiastic work of the coworkers in our research group and crystallographers who are warmly acknowledged in the relevant references. We thank Maximilian Klein for generating the TOPOS output for use in Figs. 6, 7, 8, 9 and 11.

References

1 E.C. Constable, C. E. Housecroft, Coord. Chem. Rev. (2017) doi.org/10.1016/j.ccr.2017.06.006

2 Z. Jiang, Y. Li, M. Wang, B. Song, K. Wang, M. Sun, D. Liu, X. Li, J. Yuan, M. Chen, Y. Guo, X. Yang, T. Zhang, C. N. Moorefield, G. R. Newkome, B. Xu, X. Li, P. Wang, Nature Comm. 8, 15476 (2017).

3 S. Chakraborty, W. Hong, K. J. Endres, T.-Z. Xie, L. Wojtas, C.N. Moorefield, C. Wesdemiotis, G. R. Newkome, J. Am. Chem. Soc., 139, 3012 (2017).

4 D. Liu, Z. Jiang, M. Wang, X. Yang, H. Liu, M. Chen, C. N. Moorefield, G. R. Newkome, X. Li, P. Wang, Chem. Commun., 52, 9773 (2016).

5 E. C. Constable, Coord. Chem. Rev. 252, 842 (2008).

6 J.E. Beves, D.J. Bray, J.K. Clegg, E.C. Constable, C.E. Housecroft, K.A. Jolliffe, C.J. Kepert, L.F. Lindoy, M. Neuburger, D.J. Price, S. Schaffner, F. Schaper, Inorg. Chim. Acta, 361, 2582 (2008).

7 J. E. Beves, E. C. Constable, S. Decurtins, E. L. Dunphy, C. E. Housecroft, T. D. Keene, M. Neuburger and S. Schaffner, CrystEngComm, 10, 986 (2008).

8 J. E. Beves, E. C. Constable, C. E. Housecroft, C. J. Kepert, M. Neuburger, D. J. Price, S. Schaffner and J. A. Zampese, Dalton Trans., 6742 (2008).

9 J. Yang, J.K. Clegg, Q. Jiang, X. Lui, H. Yan,W. Zhong, J.E. Beves, Dalton Trans., 42, 15625 (2013).

10 J. Yang, M. Bhadbhade, W.A. Donald, H. Iranmanesh, E. G. Moore, H. Yan, J.E. Beves, Chem. Commun., 51, 4465, (2015).

11 C. Shen, A.D.W. Kennedy, W.A. Donald, A.M. Torres, W.S. Price, J.E. Beves, Inorg. Chim. Acta , 458, 122 (2017)

12 H. Sepehrpour, M. Lal Saha, P.J. Stang, J. Am. Chem. Soc., 139, 2553, (2017).

13 E.C. Constable, Adv. Inorg. Chem., 71 (2017) in press.

14 F. Kröhnke, Synthesis 1 (1976)

15 J. Wang, G. S. Hanan, Synlett 1251 (2005).

16 M. Barquín, J. Cancela, M. J. González Garmendia, J. Quintanilla, U. Amador, Polyhedron, 17, 2373 (1998).

17 C. E. Housecroft, Dalton Trans. 43, 6594 (2014).

18 C. E. Housecroft, CrystEngComm, 17, 7461 (2015).

19 I. J. Bruno, J. C. Cole, P. R. Edgington, M. Kessler, C. F. Macrae, P. McCabe, J. Pearson, R. Taylor, Acta Cryst., B58, 389 (2002).

20 C. R. Groom, I. J. Bruno, M. P. Lightfoot, S. C. Ward, Acta Cryst. B72, 171 (2016).

21 See for example: Z. Yin, S. Zhang, S. Zheng, J.A. Golen, A.L. Rheingold, G. Zhang, Polyhedron, 101, 139 (2015); J. Grafino, R. Gavino, E. Freire, R. Baggio, Acta Cryst. C68, m269 (2012); J. Grafino, R. Gavino, E. Freire, R. Baggio, J. Mol. Struct., 1063, 102 (2014); L. Zhang, J.-D. Zheng, Y.-T. Chen, S.-R. Zheng, J. Fana, W.-G. Zhang, CrystEngComm, 17, 5538 (2015); Y. M. Klein, E. C. Constable, C. E. Housecroft, J. A. Zampese, A. Crochet, CrystEngComm, 16, 9915 (2014).

22 E. C. Constable, A. M. W. Cargill Thompson, P. Harveson, L. Macko, M. Zehnder, Chem. Eur. J., 1, 360 (1995).

23 E. C. Constable, Chem. Soc. Rev., 36, 246 (2007).

24 A. Wild, A. Winter, F. Schluetter, U. S. Schubert, Chem. Soc. Rev., 40, 1459 (2011).

25 Y. Yan, J. Huang, Coord. Chem. Rev., 254, 1072 (2010).

26 E. C. Constable, Chimia, 67, 388 (2013).

27 E. C. Constable and M.D. Ward, J. Chem. Soc., Dalton Trans., 1405 (1990).

28 G.R. Newkome, F. Cardullo, E.C. Constable, C.N. Moorefield, A.M.W. Cargill Thompson, J. Chem. Soc., Chem. Commun., 925 (1990).

29 E. C. Constable, C.E. Housecroft in J. Reedijk, ed. Elsevier Reference Module in Chemistry, Molecular Sciences and Chemical Engineering, Waltham, MA, Elsevier. doi:10.1016/B978-0-12-409547-2.13790-4

30 T.R. Cook, P.J. Stang, Chem. Rev., 115, 7001 (2015).

31 Y. M. Klein, A. Prescimone, E. C. Constable, C. E. Housecroft, CrystEngComm, 17, 6483 (2015).

32 G. W. V. Cave, C. L. Raston, J. Chem. Soc., Perkin Trans. 1, 3258 (2001).

33 S. A. S. Ghozlan, A. Z. A. Hassanien, Tetrahedron, 58, 9423 (2002).

34 J. Yoshida, S.-I. Nishikiori, H. Yuge, J. Coord. Chem., 66, 2191 (2013).

35 E. C. Constable, C. E. Housecroft, S. Vujovic, J. A. Zampese, CrystEngComm, 16, 3494 (2014); E. C. Constable, C. E. Housecroft, S. Vujovic, J. A. Zampese, CrystEngComm, 19, 2271 (2017).

36 S. Vujovic, E. C. Constable, C. E. Housecroft, C. D. Morris, M. Neuburger and A. Prescimone, Polyhedron, 92, 77 (2015).

37 D. Braga, M. Polito, D. D'Addario, E. Tagliavini, D.M. Proserpio, F. Grepioni, J.W. Steed, Organometallics, 22, 4532 (2003).

38 D. Braga, M. Polito, M. Bracaccini, D. D'Addario, E. Tagliavini, D.M. Proserpio, F. Grepioni, Chem.Commun. 1080 (2002).

39 S. R. Batten, S. M. Neville, D. R. Turner, Coordination Polymers: Design, Analysis and Application, RSC Publishing, Cambridge (2009).

40 D.-S. Li, Y.-P. Wu, J. Zhao, J. Zhang, J.Y. Lu, Coord. Chem. Rev., 261, 1 (2014).

41 S. R. Batten in Supramolecular Chemistry: From Molecules to Nanomaterials, eds. P. A. Gale, J. W. Steed, Wiley, Chichester vol. 6, p. 3107 (2012).

42 S. R. Batten, CrystEngComm, 18, 1 (2001).

43 Y.M. Klein, A. Prescimone, M. Neuburger, E.C. Constable, C.E. Housecroft *CrystEngComm*, **19**, 2894 (2017).

44 C.S. Hawes, R. Babarao, M.R. Hill, K.F. White, B.F. Abrahams, P.E. Kruger, Chem. Commun., 48, 11558 (2012).

45 J. Seo, N. Jin, H. Chun, Inorg. Chem., 49, 10833 (2010).

46 V. A. Blatov, A. P. Shevchenko, TOPOS Professional v. 4.0, Samara State University, Russia.

47 C.F. Macrae, I.J. Bruno, J.A. Chisholm, P.R. Edgington, P. McCabe, E. Pidcock, L. Rodriguez-Monge, R. Taylor, J. van de Streek, P. A. Wood, J. Appl. Cryst., 41, 466 (2008).

48 Y. M. Klein, A. Prescimone, M. B. Pitak, S. J.Coles, E. C. Constable, C. E. Housecroft, CrystEngComm, 18, 4704 (2016).

49 Y. M. Klein, A. Prescimone, E. C. Constable, C. E. Housecroft, Polyhedron, 103 (Part A), 58 (2016).

50 Y.M. Klein, A.Prescimone, E.C. Constable, C.E. Housecroft, Materials, 10, article 728 (2017).

51 Y. M. Klein, E. C. Constable, C. E. Housecroft, A. Prescimone, CrystEngComm, 17, 2070 (2015).

52 E. C. Constable, C. E. Housecroft, M. Neuburger, J. Schönle, S. Vujovic, J. A. Zampese, Polyhedron, 62, 120 (2013).

53 E. C. Constable, G. Zhang, E. Coronado, C. E. Housecroft, M. Neuburger, CrystEngComm, 12, 2139 (2010).

54 E. C. Constable, C. E. Housecroft, S. Vujovic, J. A. Zampese, A. Crochet, S. R. Batten, CrystEngComm, 15, 10068 (2013).

55 Y. M. Klein, A. Prescimone, E. C. Constable, C. E. Housecroft, Aust. J. Chem. 70, 468 (2017).

56 Y.M. Klein, A. Lanzilotto, A. Prescimone, K.W. Krämer, S. Decurtins, S.-X. Liu, E.C. Constable, C.E. Housecroft, Polyhedron, 129, 71 (2017).

57 L. Xiao, L. Zhu, Q. Zeng, Q. Liu, J. Zhang, S. Li , H. Zhou, S. Zhang, J. Wu, Y. Tian, J. Organomet. Chem., 789, 22 (2015).